Available online at www.CivileJournal.org

Civil Engineering Journal

Vol. 3, No. 2, February, 2017

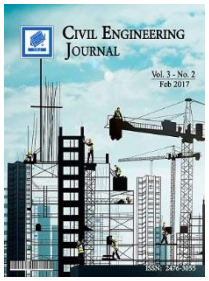

Effect of Cyclic Loadings on the Shear Strength and Reinforcement Slip of RC Beams

Mohammed A. Sakr [a*]

[a] *Assoc. Prof., Department of Structural Engineering, Tanta University, Tanta, Egypt.*

Received 21 January 2017; Accepted 25 February 2017

Abstract

Numerous studies of the response of reinforced concrete members under cyclic loadings, many of which have been summarized and have indicated that, in general, the flexural strength of under-reinforced beams remains unimpaired under cyclic loadings consisting of a reasonable number of cycles. However, there is a body of evidence indicating that their shear strength may suffer under such loadings. The first objective of the current study is to construct an accurate 2D shell finite element model of reinforced concrete beams under cyclic loadings. The second objective is carrying out a parametric study on reinforced concrete beams, using the suggested 2D shell model. The objective of this study was to observe the effect of the stirrup spacing, steel-to-concrete bond properties on the performance of reinforced concrete beams under cyclic loadings. For this purpose, an efficient and accurate finite element model was established taking into account the compression and tensile softening introducing damage in the concrete material, the Baushinger effect using nonlinear isotropic/kinematic hardening in the steel and an adequate bond-slip law for the concrete–steel interface. The simulated results of numerical models were verified by experimental results available in literature in order to validate the proposed model, including hysteretic curves, failure modes, crack pattern and debonding failure mode. The model provided a strong tool for investigating the performances of reinforced concrete beam. The results showed that: Cyclic loadings may change the failure mode of the beam to bond failure even though it has sufficient bond length to resist static loadings. So that under cyclic loadings additional anchorage length must be taken, cyclic loadings also influence the ductility and peak load for beams fail in shear. All these topics are of the utmost importance to RC behaviour to be considered by construction codes.

Keywords: Finite Element Models; Reinforced Concrete Beams; Damage; Plasticity; Cohesive Model; Cyclic Behavior.

1. Introduction

Reinforced concrete (RC) beams in general fail in two types, flexural failure and shear failure. As it known well, the shear failure of RC beam is sudden and brittle in nature. It is less predictable and so it gives no advance warning prior to failure. As a result shear failure is more dangerous than the flexural failure. It is why the RC beam must be designed to develop its full flexural capacity to assure a ductile flexural failure mode under extreme loading. However, many of RC structures are encountered shear problems due to various reasons, such as mistake in design calculations and improper detailing of shear reinforcement, construction faults or poor construction practices, changing the function of a structure from a lower service load to a higher service load, and reduction in or total loss of shear reinforcement steel area causing corrosion in service environments. Cyclic loadings in the beams of high level of shear reduce the ductility and cause brittle failure.

In service state, many engineering structures are subjected to cyclic actions. The traffic of vehicles in bridges, the wind loads on slender buildings and the wave actions in offshore structures are examples of loading with a large number of cycles acting during the life time of those structures. It is recognized and well known in the specialized literature that cyclic loads cause, in a general way, a progressive damage of the mechanical properties of structural

* Corresponding author: msakr2016@yahoo.com

materials, a progressive loss of stiffness of the structure, which is observed through the increase of deflections and cracks width in beams. In function of the number of loading cycles and the amplitude of the stresses in materials, fatigue failure can occur in the structural element.

The behaviour of reinforced concrete depends on the combined action of the concrete and its embedded reinforcement. This composite action is produced by the bond stress at the interface of the two materials. In reinforced concrete elements, the repeated cyclic loads cause the loss of steel-concrete bond, the loss of the contribution of concrete to resist tensile forces among cracks and the increase of permanent strains in materials. These effects have been extensively reported elsewhere CEB [1].

At present, the performances of reinforced concrete beam have been studied in depth by many scholars. All of them have conducted outstanding works on the behaviours of reinforced concrete beam under cyclic loadings; however, due to limited numbers of tests, the numerical simulations are widely used currently. The more accurate finite element model for parametric analysis is particularly important.

There were some reports for the numerical analysis using ABAQUS. For example, Dazio et al. [2] reported that finite element simulation was used to study and compare the cyclic behaviour of Hybrid Fibre Concrete structural walls; Aref et al. [3] proposed three dimensional cyclic meso-scale numerical procedures for simulation of unreinforced masonry structures.

However, most of these mentioned numerical simulations not focused on reinforced concrete beams. Some predictions for cyclic behaviours of reinforced concrete beams were not satisfied due to complicated contact relations and high nonlinear behaviours. For example the bond between steel reinforcement and concrete, Furthermore, the responses of steels and concrete under cyclic loadings and monotonic loadings are quite different. The traditional methods cannot accurately predict the cyclic behaviour. Therefore, an efficient and accurate finite element method should be proposed for reinforced concrete beams.

Several researchers have studied the effect of cyclic loadings on behaviour of RC beams. Crambuer et al. [4] conducted cyclic three point bending test on reinforced concrete beams. They used different loading paths in their tests, which allowed them to study relation between the hysteretic energy dissipation and damping phenomenon. Cyclic tests have been carried under various loading modes and conditions to observe different responses of materials. Liu Jin et al. [5] presented an experimental campaign on the seismic shear failure behaviour of RC cantilever beams with transverse reinforcement subjected to low-cyclic fatigue loading and found that under low-cyclic fatigue loadings, even with the transversal reinforcement, the failure of the RC beams is still brittle. Tavakoli et al. [6] studied the effects of cyclic loading rate on the mechanical behaviour of reinforced self-consolidating concrete (SCC) beams. Test results indicate that SCC beams demonstrate different behaviour before and after the yielding zone among the increase of the loading rate.

Several researchers have studied the effect of cyclic loadings on bond–slip relationships experimentally for example, Ashtiani et al. [7] studied the bond performance of steel bars in reinforced concrete members under reversed cyclic bending actions where confirmed that unlike in the monotonic test which maintained the maximum bond stress as the slip increased, the bond stress was found to reduce considerably in the beam specimen under reversed cyclic loadings once the maximum bond strength was achieved. Therefore, as opposed to the ductile bond–slip envelope observed under monotonic loadings, a substantial deterioration of bond stress occurred under cyclic loadings which can potentially have a marked influence on cyclic performance of RC structures.

Rteil et al. [8] studied the Mechanics of bond under repeated loadings and show that repeated loadings may cause fatigue failure and reduce the static capacity.

This paper deals with the deterioration of the shear strength and reinforcement bond of reinforced concrete beams under cyclic loadings with special highlighting of modelling the interaction between concrete and reinforcement. Most of the finite element models of RC beams, found in the literature, are 3D solid. Hence, the first objective of the current study is to construct an accurate 2D shell model of RC beams, the finite element models of RC beams under cyclic loading patterns were established using ABAQUS software. Element types, cyclic material constitutive models and contact models for reinforcement and concrete were proposed. Material nonlinearity was adequately considered. The numerical simulation compared well with experimental results available in literature to determine the capability of the modeling, which provided a strong tool for carrying out further analysis. The second objective of this study is carrying out a parametric study on RC beams under cyclic loadings, using the suggested 2D shell model. Different types of RC beams with various stirrup spacing and contact models for reinforcement and concrete were modelled. The carrying capacity, hysteretic behaviour and failure modes were compared and discussed comprehensively.

2. Finite Element Analysis

In order to obtain an efficient and accurate finite element method, the analysis was conducted in ABAQUS/Standard module [9]. All parts of models are presented detailedly as follows.

2.1. Element Types and Meshes

Firstly, In the modeling of concrete and steel, solid element is chosen. In general, second-order solid elements are more efficient for complex geometric and stress displacement modeling. In a reduced integration analysis procedure, first-order element acquires potentially stiffer behaviour with a slow convergence rate, preventing mesh locking and complexity. Hence, an incorporated reduced integration with the first-order 3D 8-node solid element (C3D8R) is used for steel and concrete to overcome the possible errors and to consider the cracks in tension. Such elements require a denser mesh for efficient and precise geometric simulations. However, while using reduced integration the model gets inherently stiffer, In order to save the CPU and time of analysis, only one quarter of the specimen was modelled, as shown in Figure 1. by taking advantage of the double symmetry of the beam by introducing a symmetry boundary condition along the vertical symmetric-axes of the beam. A steel loading plate and a support plate have been tied up with the concrete beam to remove the stress concentrations around the points of loading and support.

Secondly, modeling in 2D space gives the same results with high accuracy and less required time and computational capacity so the beams are modeled based on quadrilateral plane stress elements. Mesh elements consist of a four node element with reduced integration function and the reinforcements have been modeled with a 2-node linear truss element. Then, a correlation between two-dimensional (2D) and 3D finite element analyzes was established.

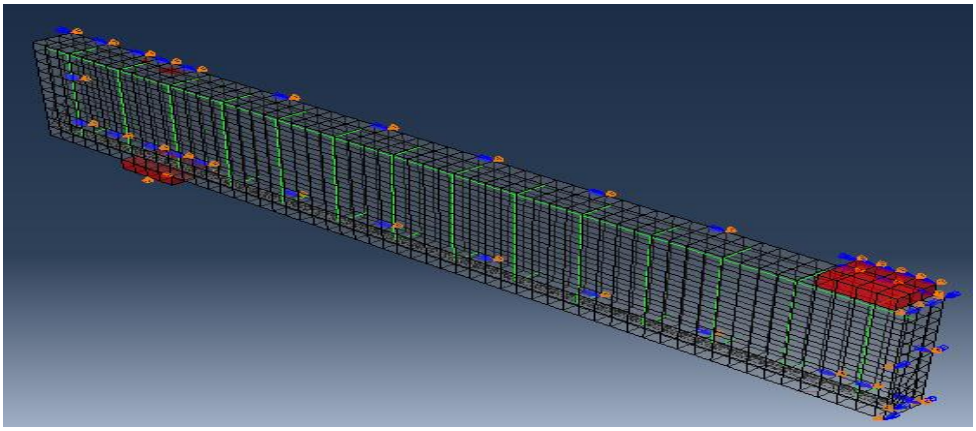

Figure 1. Boundary conditions used in numerical work for solid element

2.2. Contact Modeling

In ABAQUS reinforcement can be modeled with different methods including smeared reinforcement in the concrete, cohesive element method, discrete truss or beam elements with the embedded region constraint or built-in rebar layers. To study the effect of bond the previous numerical studies used to represent the interface between steel and concrete as a perfect bond where the reinforcements are constrained in the concrete by use of embedded region constraint, which allows each reinforcement element node to connect properly to the nearest concrete node. This type of bonding does not include the slip effects of reinforcements from concrete beam and instead, these effects were partly considered through the definition of the concrete tension softening. While in the current study the effect of bond was modeled using a cohesive zone model. The interface is modeled as a rich zone of small thickness.

Figure 2. Shows a graphic interpretation of a simple bilinear traction–separation law written in terms of the effective traction τ and effective opening displacement δ.

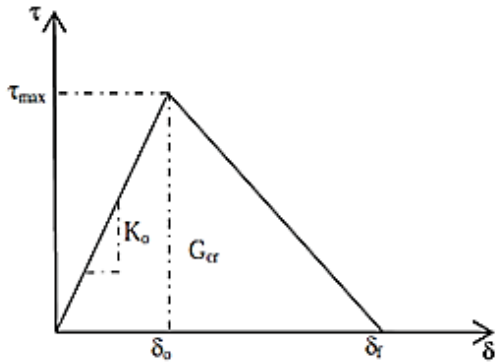

Figure 2. Bilinear traction–separation constitutive law

From Figure 2, it is obvious that the relationship between the traction stress and effective opening displacement is defined by the stiffness, K_0, the local strength of the material, τ_{max}, a characteristic opening displacement at fracture, δ_f, and the energy needed for opening the crack, G_{cr}, which is equal to the area under the traction– displacement curve. The upper limit for the maximum shear stress around bars reached in the case of deformed hooked bars. Gan, Y. [10] studied numerically the fracture energy, G_{cr}. The initiation of damage was assumed to occur when a quadratic traction function involving the nominal stress ratios reached the value one. Interface damage evolution was expressed in terms of energy release. The description of this model is available in the Abaqus material library. The dependence of the fracture energy on the mode mix was defined based on the Benzaggah–Kenane fracture criterion. Benzaggah–Kenane fracture criterion is particularly useful when the critical fracture energies during deformation purely along the first and the second shear directions are the same.

2.3. Material Modeling

2.3.1. Concrete

The mechanical properties of concrete were modeled using ABAQUS's own Concrete Damage Plasticity (CDP) formulation. The concrete compression hardening curve was fitted to the stress–strain relationship of the cylinder compression test while the concrete tension curve was fitted to the stress–displacement relationship; a key issue was the definition of the unloading and reloading branches after a tensile excursion. The parameter CONCRETE TENSION DAMAGE governing the unloading after a tensile excursion was chosen to obtain an unloading stress displacement curve as origin-oriented as possible. The recommended maximum tension damage parameter value is 0.9.

2.3.2. Steel

When steel members suffer from cyclic loadings, a steel constitutive model of cyclic plasticity is needed, which is different from the monotonic model. The constitutive model of structure steel under cyclic loadings plays a quite important role in structural seismic design and analysis. Currently, steel stress–strain relationship is commonly defined as bilinear or multi-linear forms. Those models, however, cannot satisfy cyclic loading conditions as studied by Shi Yj [11]. From Shi G study [12], a conclusion that the results calculated from cyclic model were in a better agreement with experiments for both loading and reloading processes could be obtained. The cyclic model well predicted the structural hysteretic behaviors by Shi Yj [11]. In terms of the cyclic tests of steel in Shi G study [12], the cyclic hardening criterion of steel is a combining one, containing both isotropic hardening and kinematic hardening. Chaboche [13, 14] proposed a cyclic combined model based on plastoelasticity. This model was implemented in ABAQUS as a plastic constitutive model of metal, consisting of a nonlinear kinematic hardening component and an isotropic hardening component.

The parameters of cyclic hardening according to the help files of ABAQUS are σ_{l0}, Q_∞, b_{iso}, C_{kin}, γ. where σ_{l0} is the yielding stress at zero plastic strain, Q_∞ is the maximum change in the size of yielding surface, b_{iso} is the rate at which the size of yielding surface changes as plastic straining develops, C_{kin} is the initial kinematic hardening moduli and γ is the rate at which the kinematic hardening moduli decrease with the increasing plastic deformation.

3. Verifications of Numerical Analysis

In order to validate the accuracy and applicability of non-linear finite element model of reinforced concrete beam under cyclic loadings, the typical quasi-static cyclic tests of reinforced concrete beam were selected, including the tests of Abdulridha et al. [15].

Beams B1-SM, B2-SC were loaded with a four point bending configuration with a span of 2800 mm long (2400 mm from center to center of supports), 125 mm wide and 250 mm depth and distance between loads of 125 mm. The longitudinal reinforcement consisted of two 10M bars for tension which have a nominal diameter of 11.3 mm and cross-sectional area 100 mm^2 and two smooth 6.35 mm diameter for compression. The shear reinforcement, consisting of 6.35 mm diameter closed stirrups, was spaced at 100 mm along the entire length of the beams. A concrete clear cover of 20 mm was provided throughout. Steel plates, 125 mm long, 100 mm wide, and 25 mm thick were positioned under each load to prevent local crushing of the concrete. Loading was imposed in increments of 5 kN until failure for the monotonic tests, whereas displacement control was implemented for the cyclic tests following ATC-24 [16]. The initial loading corresponded to midspan displacements starting at $0.33\Delta_y$ to Δ_y in increments of $0.33\ \Delta_y$, where Δ_y is the yield displacement. Thereafter, the loading was imposed in increments of Δ_y from Δ_y until the end of testing. Each loading cycle consisted of a single repetition. Following ATC-24, the displacement at yield, Δ_y, is 1.33 times the displacement at first yield, which is defined as the displacement corresponding to 75% of the yield load P_y.

For the two beams (B1-SM and B2-SC), initial flexural cracking was observed, for the most part, in the critical region. Flexural cracking also developed outside the critical zone, and as the load increased, inclined shear cracks were

noted near the supports. Additional shear cracks became evident with increased load, while the flexural cracking continued to propagate toward the loading points near the midspan of the beams. The first flexural crack was observed at approximately 4 kN of load. At this load level, B1-SM had crack widths of 0.1 mm in the critical zone. At yielding, the flexural cracks in B1-SM were 0.35 mm wide and spaced approximately 100 mm. prior to failure, and at a displacement ductility of approximately $7\Delta_y$ Beam B1-SM experienced a maximum crack width of 11 mm. While at a displacement ductility of 1 Δ_y, beam B2-SC recovered 30% of the crack width opening. Prior to failure, and at a displacement ductility of 6 Δ_y, the corresponding crack width recovery was approximately 21%

3.1. Material Properties and Constitutive Models

The compressive strength, f_c' was in the experimental work measured to be 34.6 MPa. E_c = 31.4 GPa. The stress–strain relationship proposed by Saenz [17] was used to construct the uni-axial compressive stress–strain curve for concrete, Poisson's ratio for concrete was assumed to be 0.2. f_{ct} were then calculated by

$$f_{ct} = 0.33\sqrt{f_c'} \approx 1.9\,MPa. \quad (1)$$

To specify the post-peak tension failure behavior of concrete the fracture energy method was used. The fracture energy for mode I, G_f, is the area under the softening curve and was assumed equal to 140 J/m^2. Accordingly, the degradation of the elastic stiffness is characterized by two damage variables, d_t and d_c. The stiffness degradation damage proposed by Jankowiak et al. [18] was used.

Parameters of cyclic hardening for steel used in ABAQUS are 425 N/mm^2, 13000.0 N/mm^2, 44.06, -200 N/mm^2, 80.0 for σ_{lo}, C_{kin}, γ, Q_∞ and b_{iso} respectively. While parameters of cohesive surface represent the interface between steel and concrete are 9.67 MPa, 30 N/mm^3 and 1200 J/m^2 for τ_{max}, K_0 and G_{cr} respectively.

3.2. Comparison of Experimental and Numerical Results

The numerical simulations agree well with test results as shown in Figures 3, 4 and 5. including monotonic curves, cyclic curves (relation between total applied load P and mid-span deflection Δ for the tested beams) and failure modes, indicating that the numerical method could accurately predict the behaviors of reinforced concrete beam. In addition, from the compared cyclic curves, phenomenon of strength degradation was well simulated.

Figure 5. provides the experimental and numerical responses of Beam B2-SC. The hysteretic behaviour was well simulated, including peak strength, ductility, residual deformations, and unloading response. Illustrate cracks compared with experimental beam, cracks that are away from the midpoint and developed due to the bending effect of the beam are at initial state for both tested beam and finite element analysis. This figure shows the contour plot of equivalent plastic strain in rebar.

The carrying capacity of Beam B2-SC mentioned was predicted. The maximum experimental and numerical imposed loads were 35 kN and 36.05 kN respectively. A good agreement between experimental and numerical results was obtained with a maximum 3% error.

For the beam B2-SC there is a big difference in the CPU time of the FE models between solid and shell elements (150 minutes for 3D solid element, 25 minutes for 2D plane stress element) It does mean the 2D plane stress model consumed about 16% of the 3D solid element CPU time. Given the minor difference of the behaviour observed among the two models, it can be state that, the 2D Plane stress element is the most suitable model for used in the parametric analysis.

Above all, the proposed finite element method could give a quite accurate prediction for the behaviors of reinforced concrete beams under cyclic loadings.

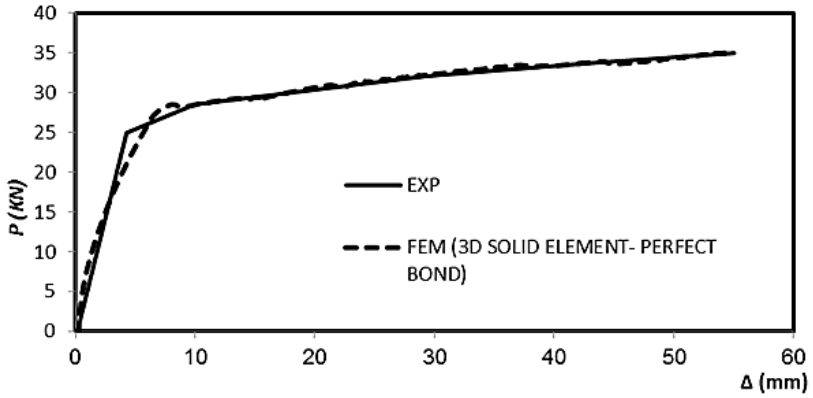

Figure 3. The monotonic curves

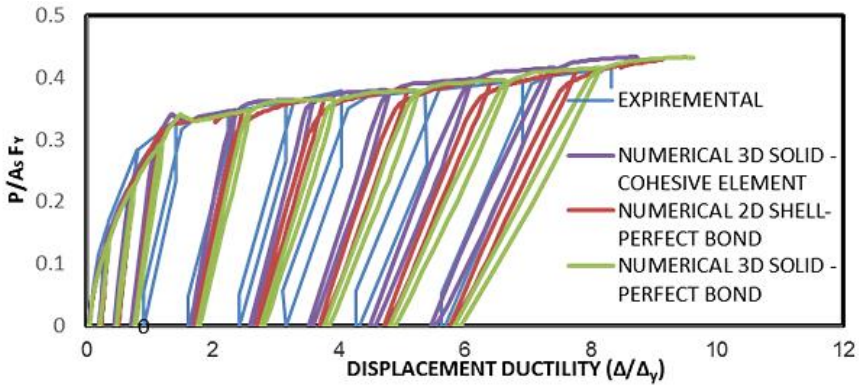

Figure 4. The cyclic curves

Figure 5-a. Failure condition of beam B2-SC

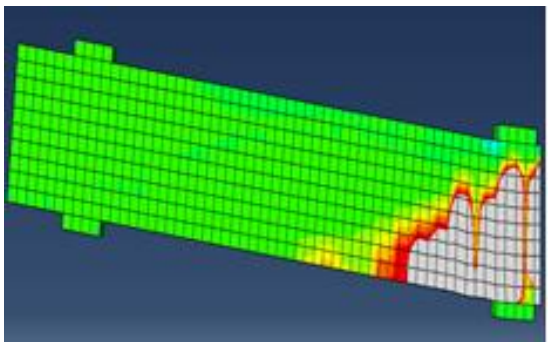

Figure 5-b. Plastic strain distribution for 3d model

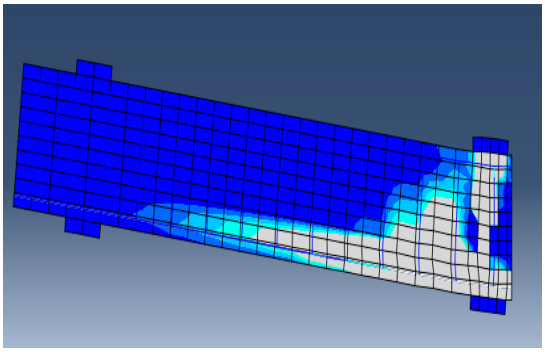

Figure 5-c. Plastic strain distribution for 2d model

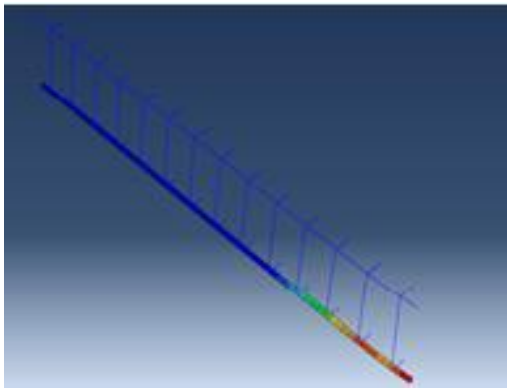

Figure 5-d. Plastic strain contour plot for 3d model

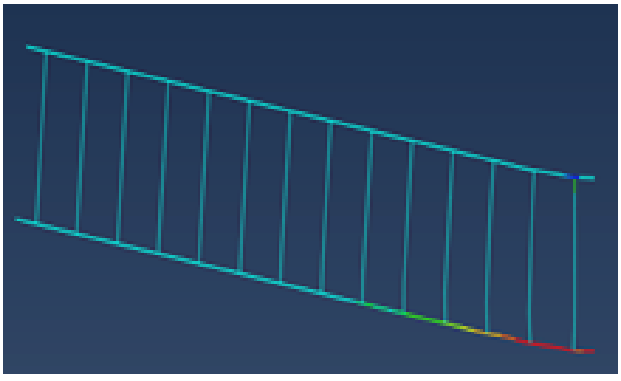

Figure 5-e. Plastic strain contour plot for 2d model

Figure 5. Experimental failure condition and numerical plastic strain distribution

4. Parametric Analysis

To show the effect of cyclic loadings on the shear strength and the reinforcement slip of RC beam, a finite element failure analysis of 2D shell elements have been developed under monotonic and cycling loadings using Abaqus program. Analysis was performed to model the nonlinear behavior of the beams with geometry and reinforcement as shown in Figure 6. All beams have the same overall cross-sectional dimensions, internal longitudinal reinforcement. The beams are 150 *mm* wide, 300 *mm* high and 1700 *mm* long, the net span equal 1500 *mm*. For all concrete beams, the hanging region width was chosen to be 200 *mm* that gives sufficient bond length to prevent debonding according the design codes. Three types of the mild steel bars (Low Carbon Steel) were used for the longitudinal and the transverse reinforcements. There were two sets of steel mild bars placed in the tensile and compressive faces of the beam respectively. There were also steel smooth bars placed transversely for the shear reinforcement. The details of the reinforcement and material properties of the rebar and concrete are summarized in Figure 6. and Table 1, respectively. Displacement control was implemented for the monotonic and cyclic tests following ATC-24 [16].

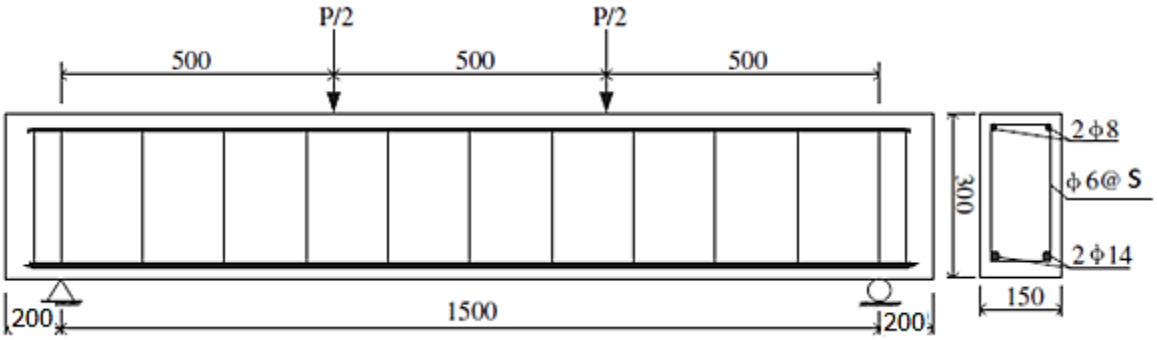

Figure 6. The geometric, loading and boundary conditions and steel reinforcement of the RC beams

Table 1. Mechanical properties of the RC beams

Material	Dimensions (mm)	Yield strength (MPa)	Compressive strength (MPa)	Tensile strength (MPa)	Elastic modulus (GPa)	Ultimate strain (%)
Concrete	C30	–	31.3	–	–	0.25
Steel	D = 6	240	–	420	210	30.0
		σ_{Io} = 240 N/mm^2 , C_{kin} = 56760.0 N/mm^2 , γ = 420 , Q_{∞} = 77 N/mm^2 , b_{iso} = 10.5				
	D = 8	330	–	490	210	28.0
		σ_{Io} = 330 N/mm^2 , C_{kin} = 7993.0 N/mm^2 , γ = 175 , Q_{∞} = 21 N/mm^2 , b_{iso} = 1.20				
	D = 14	410	–	555	200	28.5
		σ_{Io} = 410 N/mm^2 , C_{kin} = 13000 N/mm^2 , γ = 44.06 , Q_{∞} = -200 N/mm^2 , b_{iso} = 80.0				

Note: σ_{Io}, C_{kin}, γ, Q_{∞} and b_{iso} are the parameters of cyclic hardening for steel used in ABAQUS

Only half of the beam has been modeled because of symmetrical condition by introducing a symmetry boundary condition along the vertical symmetric-axis of the beam. A steel loading plate and a support plate have been tied up with the concrete beam to remove the stress concentrations around the points of loading and support. All the reinforcements have been modeled with truss elements (Type T2D2) according to their respective yield or rupture strengths. The beams are modeled based on quadrilateral plane stress elements. Mesh elements consist of a four node element with reduced integration function known as CPS4R with an element mesh size of 28×25 *mm* (in horizontal and vertical directions respectively). Figure 7. shows the geometry and boundary conditions of the concrete beam model. Table 2. shows the number of elements, number of degrees of freedom.

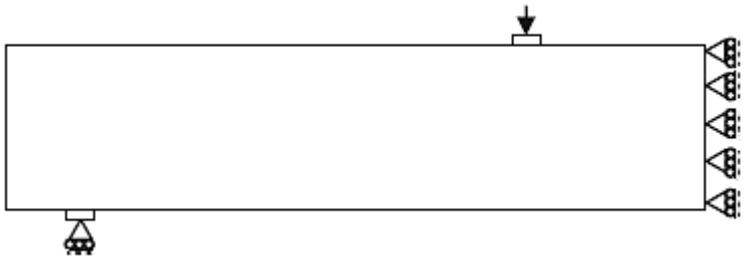

Figure 7. Boundary conditions used in numerical work

Table 2. Model size

Model	Number of shell elements	Number of truss elements	Total number of elements	Number of degrees of freedom (DOF)
Beam with stirrup spacing 150 mm / embedded region	416	116	532	1064

4.1. The Effect of Cyclic Loadings on the Shear Strength

In this part, just embedded region (perfect bond) modeling used for reinforcement. According to Hibbit et al [9]. The effect of bond slip is not considered in the embedded region modeling method but this effect is considered somewhat by definition of the tension stiffening behavior of concrete. Figures 8 and 9. show load–deflection curves for beams with stirrup spacing varied from 75 mm to 200 mm under monotonic and cyclic loadings respectively. Clearly the stirrup spacing has a significant effect on the value of ultimate load and the post-peak behavior of all beams but a very small effect on the pre-peak behavior. It was shown that in both monotonic and cyclic tests decreasing the stirrup spacing resulted in a substantial increase in the peak load and also enhanced significantly the ductility, cyclic loadings causing significant reduction on the peak load (shear strength) and ductility due to significant accumulation on plastic deformation. An explanation of such behavior may be found in the progressive deterioration of concrete under cyclic loadings, in addition, increasing stirrup spacing lead to wider openings and deeper cracks for the same applied load. As shown in Figure 10. The predicted failure modes are ductile flexural failure for beams with stirrup spacing 75 and 125 mm and brittle shear failure for beam with stirrup spacing 150 mm. From Figure 10-e and 10-f, the plastic strain was different from the monotonic and cyclic loadings.

Defining the level of ductility as the ratio between the deflection at the maximum load and the deflection at the yielding of the longitudinal steel bars (δ_{max}/δ_y). Summary of numerical results were shown in Table 3.

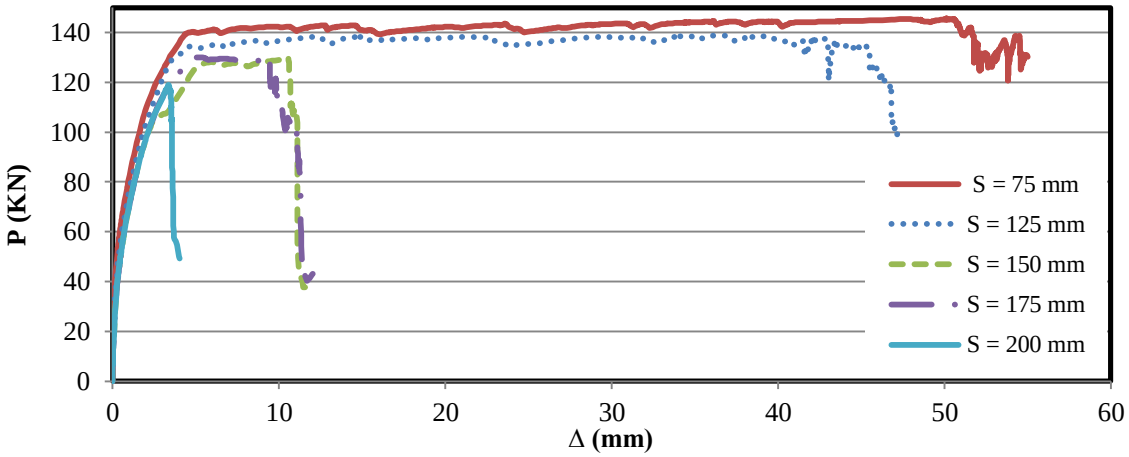

Figure 8. The monotonic curves (Full bond)

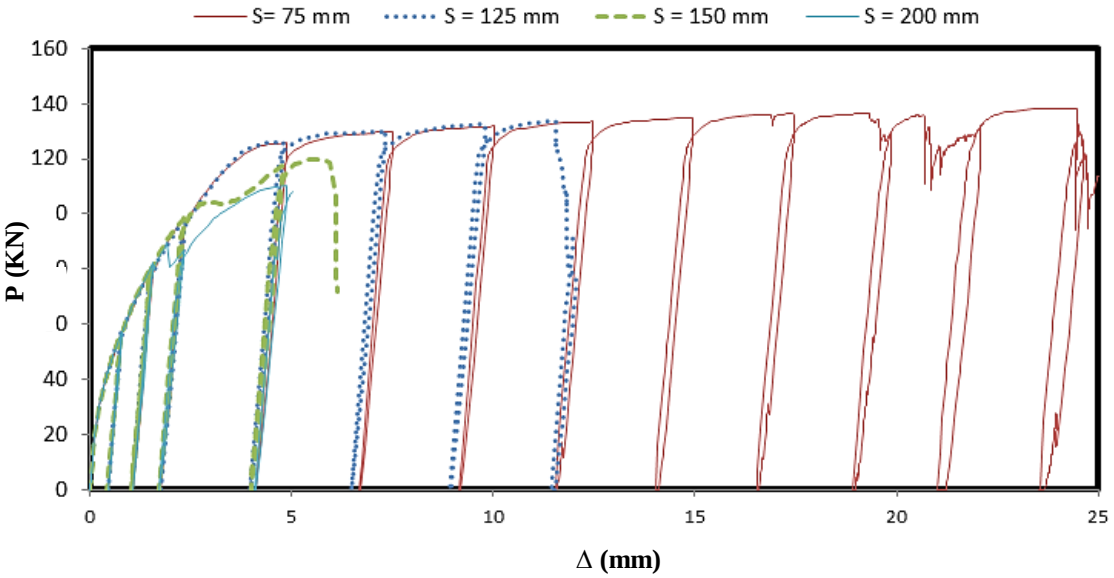

Figure 9.The cyclic curves (Full bond)

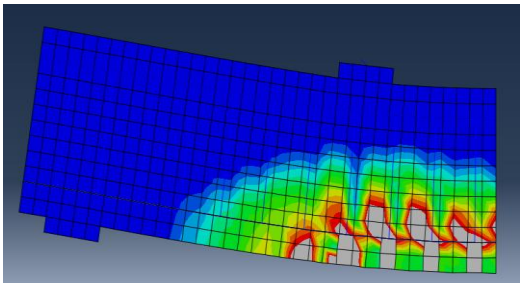

Figure 10-a. Plastic strain distribution with stirrup spacing 75 mm under monotonic loading at maximum load =140 kN

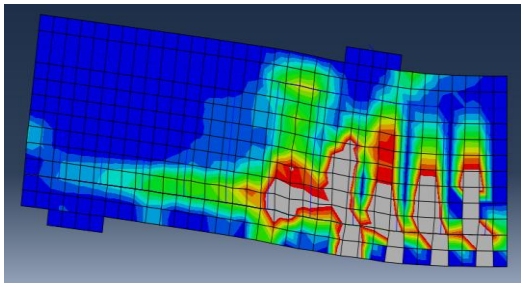

Figure 10-b. Plastic strain distribution with stirrup spacing 75 mm under cyclic loading at maximum load = 136 kN

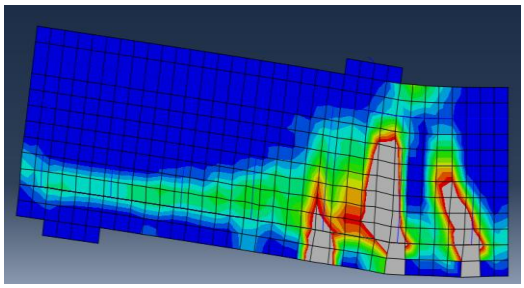

Figure 10-c. Plastic strain distribution with stirrup spacing 125 mm under monotonic loading at maximum load = 138 kN

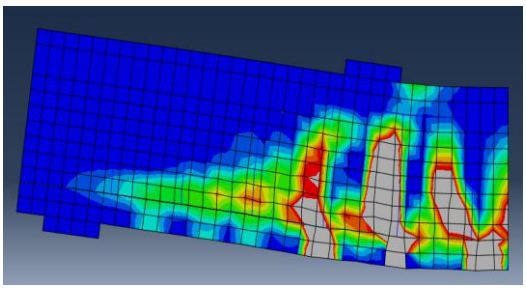

Figure 10-d. Plastic strain distribution with stirrup spacing 125 mm under cyclic loading at maximum load =133 kN

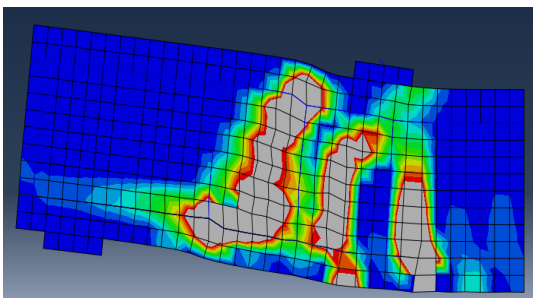

Figure 10-e. Plastic strain distribution with stirrup spacing 150 mm under monotonic loading at maximum load = 128 kN

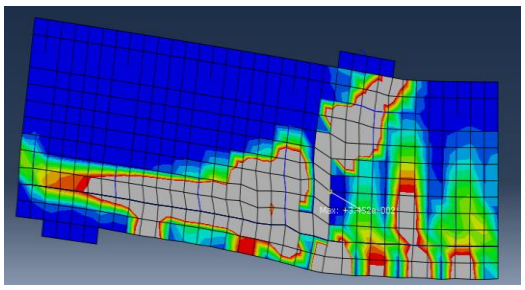

Figure 10-f. Plastic strain distribution with stirrup spacing 150 mm under cyclic loading at maximum load = 120 kN

Figure 10. Plastic strain distribution

Table 3. Comparison between monotonic and cyclic behaviour of beams with different stirrup spacing

Stirrup spacing	P_u (kN)		% Reduction of ultimate load	Δ_y (mm)		Δ_u (mm)		Ductility (Δ_y / Δ_u)		% Reduction of cyclic ductility	Failure mode	
	Static	Cyclic		Static	Cyclic	Static	Cyclic	Static	Cyclic		Static	Cyclic
75	140	136	2.85	4	4.9	55	24.6	13.75	5.02	63.5	Flexural	Flexural
125	138	133	3.6	4.2	5.1	45	10	10.7	1.96	81.7	Flexural	Flexural
150	128	120	6.25	4.4	5.4	10.6	5.5	2.4	1.01	57.9	Shear	Shear
200	120	110	8.3	---	---	---	---	---	---	---	Shear	Shear

4.2. The Effect of Cyclic Loadings on the Reinforcement Slip

In this part to show the effect of the bond model, the shear reinforcement, consisting stirrups, was spaced at 150 mm along the entire length for all beams. Taking interfacial shear = 9.67 MPa as a suitable value according to Gan, Y. [10] and to investigate to what extent G_{cr} (fracture energy of interfacial shear) affects the results three cohesive bond models were tested under monotonic loadings with interfacial shear = 9.67 MPa, K_0 equal 30 N/mm^3 and G_{cr} equal zero J/m^2, 250 J/m^2 and 1200 J/m^2 respectively and the results shown in Figure 11.

Figure 11. also confirmed that stronger interfaces lead to narrower openings and shorter cracks for the same applied load. Therefore, shear failure tends to disappear as bond strength increases because a stronger bond leads the flexural steel bars to yield before the crack reaches the critical depth thereby causing shear failure.

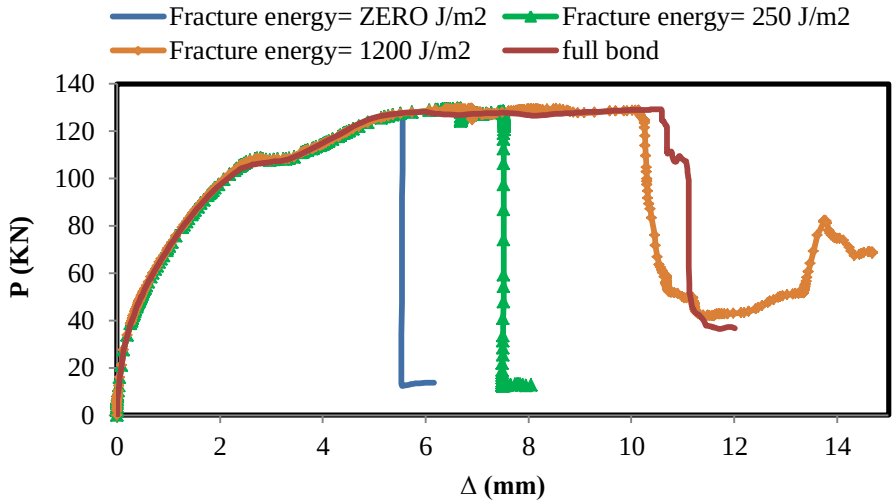

Figure 11. Load-displacement curves for different fracture energies (Interfacial shear = 9.67 MPa)

Figure 12. shows the load–displacement behavior of the cyclic beam tests in comparison with the monotonic tests. In both monotonic and cyclic tests, load–displacement relationship followed almost the same path as long as the response was in the linear phase. In the nonlinear phase the load continued to increase in the monotonic tests and it peaked at around 129 kN for perfect bond model and 128 kN for cohesive model at a displacement of about 10.3 mm and 10 mm respectively, after which the beam started to deteriorate. Under monotonic tests the failure mode was a typical shear failure, i.e. the failure occurred suddenly by formation of a diagonal crack near the support propagating to a loading point, as shown in Figure 13-a.

However, in the cyclic test the effect of load started deteriorating the bond between steel and concrete after the first three cycles of 3 mm displacement, when the bond stress reached its maximum value of about 9.67 MPa and the slip was about 0.3 mm. In the nonlinear phase the load continued to increase in the cyclic tests and it peaked at around 119.6 kN for perfect bond model and 107.9 kN for cohesive model at a displacement of about 5.8 mm, 3.6 mm, respectively. In the subsequent cycles, as the number of cycles increased, a longitudinal crack initiated and propagated at the loaded end of the shear zone from the bottom of the beam. This crack continued to increase in length and width until final failure of the beam by bond in spite of the bond length is sufficient to prevent debonding according to design codes. Overall, the ultimate load levels were significantly higher in the monotonic; mainly because of more bond deterioration in the cyclic test. As shown in Figure 12. cyclic loadings have significant effect on ultimate

capacity and displacement which have been decreased compared with static loadings by 15.7% and 64%, respectively when using the cohesive surface model.

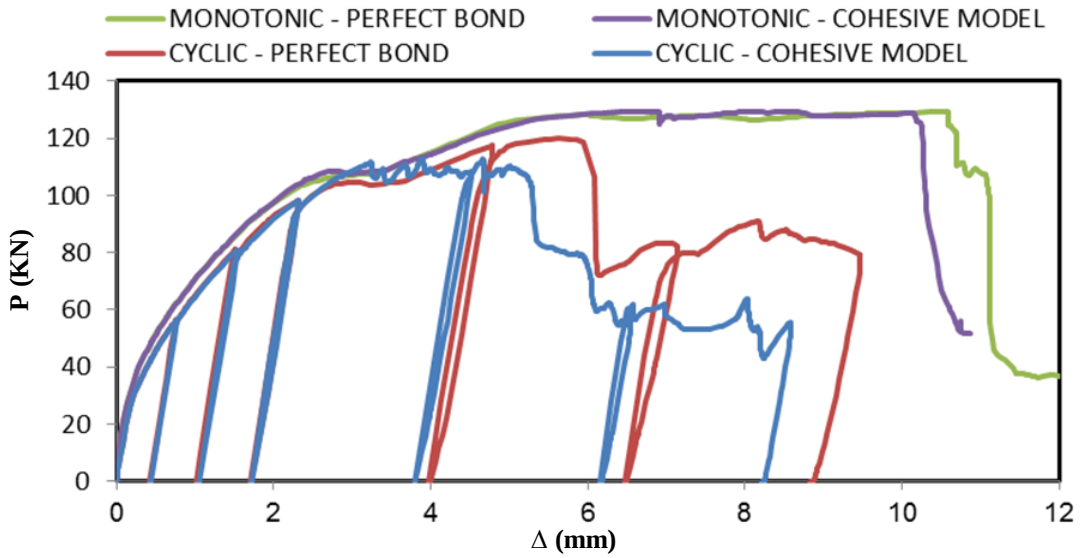

Figure 12. Load-displacement curves for different model of interfacial behaviour under monotonic and cyclic loadings

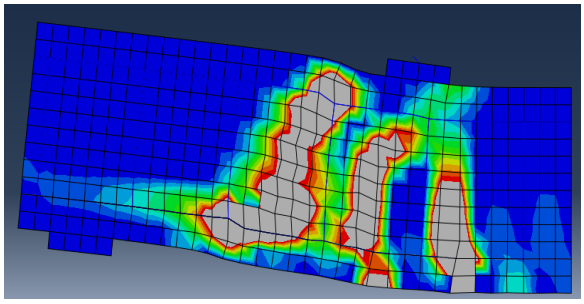

Figure 13-a Plastic strain distribution with stirrup spacing 150 mm under monotonic loading (Cohesive model)

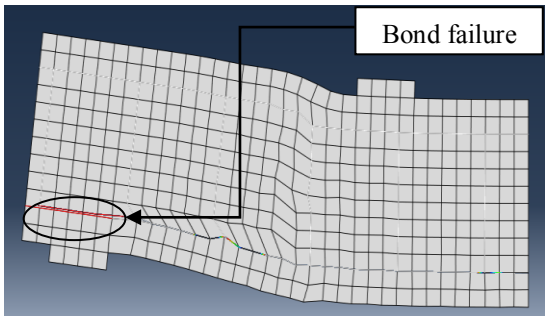

Figure 13-b Debonding of reinforcement for beam with stirrup spacing 150 mm under cyclic loading (Cohesive model)

Figure 13. Debonding and plastic strain distribution under monotonic and cyclic loadings

To show the effect of bond length in the hanging region on reinforced concrete beam under cyclic loadings (i.e., the part of the beam outside the support) two beams was considered with stirrups spaced at $150\,mm$ along the entire length, the first beam with straight bottom reinforcement ended at the beam ends and the second beam with L-shaped reinforcement with vertical length equal $0.9d$ (d effective depth of the beam) which represent additional anchorage length in the hanging region. Figure 14. shows the load–displacement behavior of the two cyclic beams for different shape of main reinforcements. The results showed that, even the beam had a sufficient bond length according to design codes, bond failure occurred at the end of the beam due to the effect of cyclic deterioration. While in the second beam using L shape ending prevent end debonding and the beam failed in shear. So it is recommended to use L shape end for main reinforcement in the hanging region of simply supported RC beams subjected to cyclic loadings.

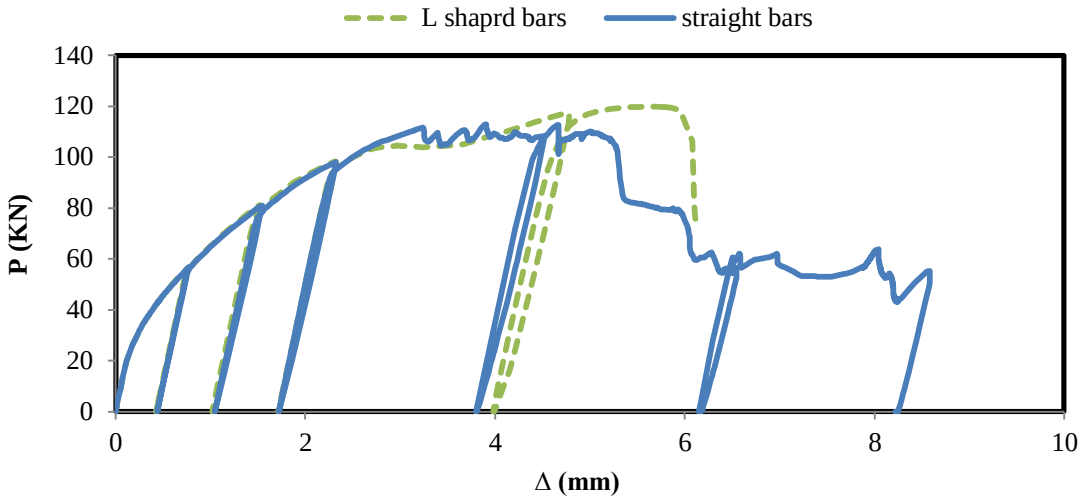

Figure 14. Comparison between cyclic analysis results for different shapes of main reinforcements

5. Conclusions

The nonlinear finite element method of reinforced concrete beam under cyclic loadings was established, which was verified by typical test results. Comparative analyses of beams with different stirrup spacing and different bond model were carried out. The following conclusions can be drawn:

- The proposed finite element model could give a quite accurate prediction for the behaviors of reinforced concrete beams under cyclic loadings taking the effect of interface between reinforcement, compression and tensile softening introducing damage in the concrete material and the Baushinger effect using nonlinear isotropic/kinematic hardening in the steel, including carrying capacity, hysteretic curves and failure modes. It proved the rationality of selected element types, constitutive models and contact models. The finite element model provided a strong tool for studying the performance of reinforced concrete beams.
- For beams fail in shear, cyclic loadings causing significant reduction on the peak load (shear strength) and ductility due to significant accumulation on plastic deformation. The reduction of ultimate load reached to 8.3% based on the numerical results of the current study.
- The numerical analysis reported on the present paper evidence the high influence of the cyclic loadings on the bond-slip behavior and on the ultimate capacity and displacement of RC simply supported beams. Cyclic loadings compared with monotonic loadings may change the mode of failure from shear to anchorage debonding.
- Under cyclic loadings, the results showed that, for RC beams have sufficient anchorage bond length according to design codes, bond failure may occur at the end of the beam. So additional anchorage length in the hanging region must be taken or using L shape ending to prevent end debonding.

6. References

[1] Du Beton, Comite Euro-Internationale. “Elements under Cyclic Loading: State of the Art Report.” Tomas Telford, London, UK (1996): n. pag.

[2] Crambuer, R., B. Richard, N. Ile, and F. Ragueneau. "Experimental characterization and modeling of energy dissipation in reinforced concrete beams subjected to cyclic loading." Engineering Structures 56 (2013): 919-934.

[3] Jin, Liu, Xiuli Du, Dong Li, and Xiao Su. "Seismic behavior of RC cantilever beams under low cyclic loading and size effect on shear strength: An experimental characterization." Engineering Structures 122 (2016): 93-107.

[4] Tavakoli, H. R., S. Mahmoudi, A. R. Goltabar, and P. Jalali. "Experimental evaluation of the effects of reverse cyclic loading rate on the mechanical behavior of reinforced SCC beams." Construction and Building Materials 131 (2017): 254-266.

[5] Dazio, Alessandro, Davide Buzzini, and Martin Trüb. “Nonlinear Cyclic Behaviour of Hybrid Fibre Concrete Structural Walls.” Engineering Structures 30.11 (2008): 3141–3150.

[6] Aref, Amjad J, and Kiarash M Dolatshahi. “A Three-Dimensional Cyclic Meso-Scale Numerical Procedure for Simulation of Unreinforced Masonry Structures.” Computers & Structures 120 (2013): 9–23.

[7] Ashtiani, M Soleymani et al. “Cyclic Beam Bending Test for Assessment of Bond--Slip Behaviour.” Engineering Structures 56

(2013): 1684–1697.

[8] Rteil, Ahmad, Khaled Soudki, and Timothy Topper. "Mechanics of Bond under Repeated Loading." Construction and Building Materials 25.6 (2011): 2822–2827.

[9] Hibbitt, Karlsson. "Sorensen, Inc. ABAQUS Theory Manual." 2000: n. pag.

[10] Gan, Youai. "Bond Stress and Slip Modeling in Nonlinear Finite Element Analysis of Reinforced Concrete Structures." University of Toronto, 2000.

[11] Shi, Yongjiu, Meng Wang, and Yuanqing Wang. "Experimental and Constitutive Model Study of Structural Steel under Cyclic Loading." Journal of Constructional Steel Research 67.8 (2011): 1185–1197.

[12] Shi, Gang et al. "Experimental and Modeling Study of High-Strength Structural Steel under Cyclic Loading." Engineering Structures 37 (2012): 1–13.

[13] Chaboche, Jean-Louis. "Time-Independent Constitutive Theories for Cyclic Plasticity." International Journal of Plasticity 2.2 (1986): 149–188.

[14] Chaboche, Jean-Louis. "Constitutive Equations for Cyclic Plasticity and Cyclic Viscoplasticity." International journal of plasticity 5.3 (1989): 247–302.

[15] Abdulridha, Alaa et al. "Behavior and Modeling of Superelastic Shape Memory Alloy Reinforced Concrete Beams." Engineering Structures 49 (2013): 893–904.

[16] ATC, A T C. "24, Guidelines for Cyclic Seismic Testing of Components of Steel Structures." Redwood City, CA: Applied Technology Council (1992): n. pag.

[17] Saenz, L P. "Equation for the Stress-Strain Curve of Concrete." ACI J 61.9 (1964): 1229–1235.

[18] Jankowiak, Tomasz, and Tomasz Lodygowski. "Identification of Parameters of Concrete Damage Plasticity Constitutive Model." Foundations of civil and environmental engineering 6.1 (2005): 53–69.